

J. MARCINKOWSKI (Wrocław)

## STATICAL MOMENTS OF EXACT AND APPROXIMATE PROFILES OF AIR SPRINGS

**1. Introduction.** Air springs have usually the shape of rotational solids. It may be assumed that the inside pressure of gas induces such a shape of the spring which insures its maximal volume, given the area of its surface. This statement leads to a variational problem which was studied in the author's earlier paper [7]. Obviously the meridian section of the spring is a plane domain symmetrical with respect to the axis of rotation, which may be taken as the  $y$ -axis. It was proved in [7] that it is symmetrical with respect to the  $x$ -axis as well. Its part  $D$  lying in the quarter  $x > 0, y > 0$  (Fig. 1) is bounded by a line  $\Gamma$  (called by the author anti-ellipse) and by two segments:  $[x_1, x_2]$

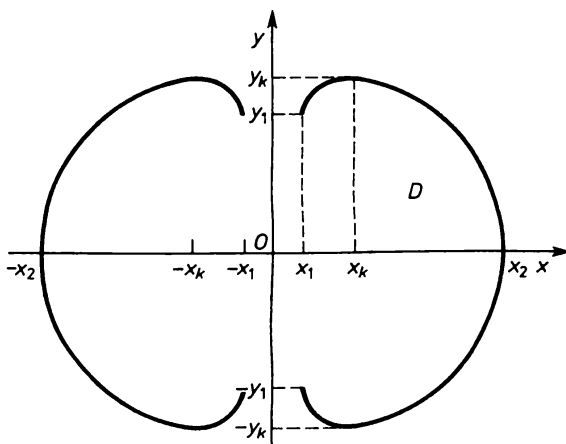


Fig. 1

of the  $x$ -axis and  $[0, y_1]$  of the line  $x = x_1$ . The line  $\Gamma$  is described by the equation

$$(1) \quad y = \int_{x_2}^x \frac{x_k^2 - x^2}{\sqrt{w(x)}} dx,$$

where

$$w(x) = -x^4 + 2x^2(x_k^2 + 2\lambda^2) - x_k^4,$$

or, equivalently,

$$w(x) = -x^4 + x^2(x_1^2 + x_2^2) - x_1^2 x_2^2,$$

$x_1$  and  $x_2$  ( $x_1 < x_2$ ) are the abscissas of the two endpoints of the anti-ellipse  $\Gamma$ ;

$$(2) \quad x_k = \sqrt{x_1 x_2}$$

is the mean distance of  $\Gamma$  to the  $y$ -axis;

$$\lambda = \frac{1}{2}(x_2 - x_1)$$

is the half-diameter of  $\Gamma$ .

We put also  $y_j = y(x_j)$ , for  $j = 1, 2, k$ , where  $y$  denotes the function defined by (1); note that  $y_2 = 0$ .

The line  $\Gamma$  was obtained as an extremal of the following variational problem: find the line  $AB$  with given statical moment<sup>(1)</sup> in such a way that the statical moment of the domain  $D$  should be a maximal one.

As the Euler equation, which was the basis of the investigations [2], gives only the necessary condition for the extremum of the functional we complete our earlier result by a numerical study of the problem and this is the aim of the present paper.

It is usually assumed in technical investigations that the meridian section of a fold of the air spring is an arc of a circle. We are going to show in this paper that this supposition, although well justified in practical considerations, is not exact.

Unfortunately, it is very inconvenient to compare the numerical values of the statical moments of the two domains bounded by the anti-ellipse and by the circle, respectively. Numerical experiments performed by the author have shown that their difference, assuming the statical moments of the corresponding lines be equal, does not exceed the computation error.

---

<sup>(1)</sup> By "statical moment" we understand in this paper the statical moment with respect to the  $y$ -axis.

Therefore we shall construct in Section 5 an arch curve  $\Gamma_p$  (Fig. 5), consisting of arcs of two circles, with the following properties:

(i) The computation error of the statical moments of  $\Gamma_p$  and of the domain  $D_p$  bounded by it depends only on the assumed computation accuracy of the number  $\pi$ .

(ii)  $\Gamma_p$  is in some sense (which will be precised below) more close to the anti-ellipse  $\Gamma$  than is the arc  $C$  of a circle.

In Section 5 we give an example of the lines  $\Gamma_p$  and  $C$ , having approximately the same statical moments  $T_p$  and  $T_c$  and for which the difference  $U_p - U_c$  of statical moments of the corresponding domains is positive. This difference equals about 2<sup>0</sup>/<sub>0</sub> of the values  $U_p$  and  $U_c$ , but does exceed more than 100 times the computation error.

In the sequel we describe a graphical method convenient to calculate the parameters  $x_1$  and  $x_2$  of the anti-ellipse with given axis of rotation and going through a given point. We prove also that, considering the values of the tensions of the shell, we may replace an arc of the anti-ellipse by a suitable arc of a circle.

**2. Some auxiliary functions.** We need in the sequel the following two functions:

$$(3) \quad z(x) = - \int_{x_2}^x \frac{x_k^2 + x^2}{\sqrt{w(x)}} dx$$

and

$$(4) \quad j(x) = \int_{x_2}^x \sqrt{w(x)} dx.$$

The graph of function  $z(x)$  has some properties similar to those of the line  $\Gamma$  described by (1). Its length  $l_z$  may be expressed by elementary functions and its radius of curvature  $R_z$  is a rational function of  $x$ . We have thus

$$l_z(x) = (x_2 + x_1) \arcsin \sqrt{\frac{x_2^2 - x^2}{x_2^2 - x_1^2}}$$

and

$$R_z(x) = \frac{x^2(x_2 + x_1)}{x^2 - x_1 x_2}.$$

Remind that for the line  $\Gamma$  the corresponding expressions for  $l$  and  $R$  are, according to [7],

$$(5) \quad l(x) = (x_2 - x_1) \arcsin \sqrt{\frac{x_2^2 - x^2}{x_2^2 - x_1^2}}$$

and

$$R(x) = \frac{x^2(x_2 - x_1)}{x^2 + x_1 x_2},$$

so

$$l_z(x) = \frac{x_2 + x_1}{x_2 - x_1} \cdot l.$$

The approximative values of function  $z$  may be expressed in a similar way as it was done in [7] for the function  $y$  given by (1) or in terms of elliptic integrals [4], as follows:

$$z = x_2 E(\varphi, k) + x_1 F(\varphi, k).$$

We have sketched on Figure 2 the graphs of the functions  $y$  and  $z$  with identical parameters  $x_k$  and  $\lambda$ .

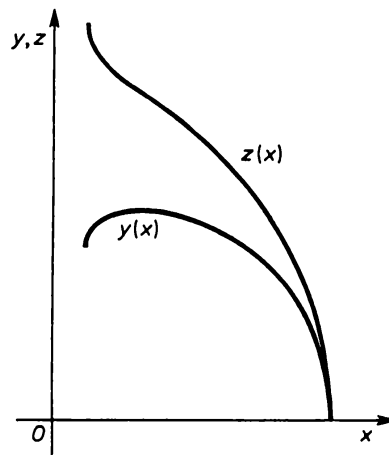


Fig. 2

Concerning the function  $j$ , its values may be computed approximately by numerical integration, because the integrand in (4) is bounded in the whole interval  $[x_1, x_2]$ . It may be expressed also by elliptic integrals [3].

**3. Evaluation of statical moments of the anti-ellipse.** The statical moment  $T_y$  of the part  $\Gamma_{AB}$  of the anti-ellipse is given by

$$T_y = \int_A^B x \, dl,$$

or, equivalently, by

$$(6) \quad T_y = \int_{x_A}^{x_B} x \sqrt{1 + y'^2} \, dx.$$

Calculating  $y'$  from (1) yields

$$T_y = 2 \int_{x_A}^{x_B} \frac{x^2}{\sqrt{w(x)}} \, dx;$$

thus

$$T_y = -\lambda(y+z) \Big|_{x_A}^{x_B}.$$

We need also the statical moment of the plane domain  $D_{AB}$  bounded by arc  $\Gamma_{AB}$  and by the line segments  $x = x_A$ ,  $x = x_B$  and  $y = y_A$  (Fig. 3).

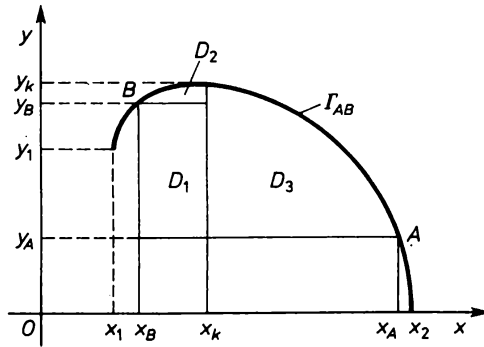


Fig. 3

The usual expression for the statical moment of a domain will be brought to a form convenient in further numerical calculations. It was shown in [7] that  $y$  defined by (1) is a strictly increasing function in the interval  $[x_1, x_k]$ , takes its maximum value  $y_k$  in the point  $x_k$  and decreases in the interval  $[x_k, x_2]$ . The two parts of the anti-ellipse corresponding to the intervals  $[x_1, x_k]$  and  $[x_k, x_2]$  can be described by the equations

$$\text{or} \quad \begin{aligned} x &= g_1(y), & y_1 &\leq y \leq y_k, \\ x &= g_2(y), & y_A &\leq y \leq y_k, \end{aligned}$$

respectively (see Fig. 3). The domain  $D_{AB}$  consists of three parts  $D_j$ ,  $j = 1, 2, 3$ , described as follows (Fig. 3):

$$\begin{aligned} D_1: & \quad y_A \leq y \leq y_B, \\ & \quad x_B \leq x \leq x_k; \\ D_2: & \quad y_B \leq y \leq y_k, \\ & \quad g_1(y) \leq x \leq x_k; \\ D_3: & \quad y_A \leq y \leq y_k, \\ & \quad x_k \leq x \leq g_2(y). \end{aligned}$$

Then the statical moment  $U_y$  of the domain  $D_{AB}$  equals

$$\iint_{D_{AB}} x \, dD = \sum_{j=1}^3 \iint_{D_j} x \, dD.$$

Performing the integration with respect to  $x$  in the integrals on the right we obtain

$$\begin{aligned} \iint_{D_1} x \, dD &= \frac{1}{2} \int_{y_A}^{y_B} (x_k^2 - x_B^2) \, dy, \\ \iint_{D_2} x \, dD &= \frac{1}{2} \int_{y_A}^{y_k} (x_k^2 - g_1(y)) \, dy, \\ \iint_{D_3} x \, dD &= \frac{1}{2} \int_{y_A}^{y_k} (g_2^2(y) - x_k^2) \, dy, \end{aligned}$$

and this yields

$$2 \iint_{D_{AB}} x \, dD = \int_{y_A}^{y_k} g_2^2(y) \, dy - \int_{y_B}^{y_k} g_1^2(y) \, dy - x_B^2 (y_B - y_A).$$

Substituting (1) in the integrals on the right-hand side we get

$$\int_{y_B}^{y_k} g_1^2(y) \, dy = - \int_{x_k}^{x_B} x^2 y'(x) \, dx$$

and

$$\int_{y_A}^{y_k} g_2^2(y) \, dy = \int_{x_A}^{x_k} x^2 y'(x) \, dx,$$

so finally

$$U_y = \frac{1}{2} \int_{x_A}^{x_B} x^2 y' \, dx - \frac{1}{2} x_B^2 (y_B - y_A).$$

Calculating  $y'$  from (1) yields now

$$U_y = \frac{1}{2} \int_{x_A}^{x_B} \frac{(x_k^2 - x^2)x^2}{\sqrt{w(x)}} dx - \frac{1}{2} x_B^2 (y_B - y_A)$$

or equivalently, making use of formulas (1), (3) and (4),

$$U_y = [\lambda^2 z + (\frac{1}{2} x_k^2 + \lambda^2) y + \frac{1}{2} j]_{x_A}^{x_B} - \frac{1}{2} x_B^2 (y_B - y_A).$$

As it is well known

$$(7) \quad U_y = Sx_s,$$

where  $S$  denotes the area of domain under consideration and  $x_s$  is the  $x$ -coordinate of its centre of gravity. Identity (7) allows to verify in a simple manner the numerical calculations of  $U_y$ . We have namely to make a model of the domain, using a piece of stiff cardboard and then one can find the line  $x = x_s$  of the centre of gravity putting this model on the edge of a knife. The error of such an experimental measurement equals about 0.1 cm.

**4. Substitution of an arc of the anti-ellipse by an arc of a circle.** We substitute in this section a given arc  $\tilde{\Gamma}$  of the anti-ellipse by a suitably constructed arc of a circle with identical statical moments and then try to compare the statical moments of the corresponding domains (Fig. 4a).

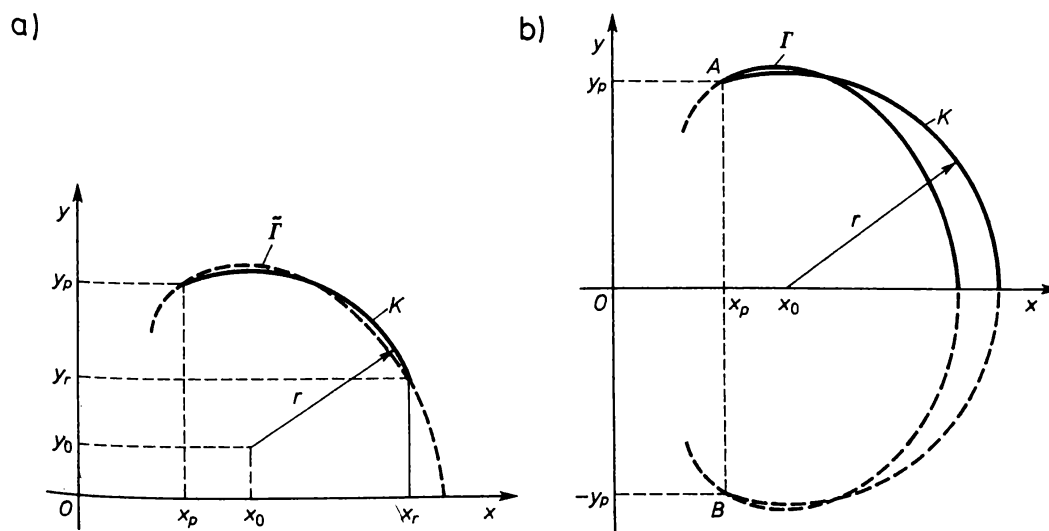


Fig. 4

Let us consider the circle with centre  $(x_0, y_0)$  and radius  $r$ ; its equation

$$(8) \quad (x - x_0)^2 + (y - y_0)^2 = r^2,$$

and therefore

$$1 + y'^2 = \frac{r^2}{r^2 - (x - x_0)^2}.$$

According to (6) we obtain for the static moment of the arc  $K$  of (8) with end points  $(x_p, y_p)$  and  $(x_r, y_r)$ :

$$T_{yK} = \int_{x_p}^{x_r} \frac{rx}{\sqrt{r^2 - (x - x_0)^2}} dx$$

or, after evaluation of the integral,

$$(9) \quad T_{yK} = rx_0 \left( \arcsin \frac{x_r - x_0}{r} - \arcsin \frac{x_p - x_0}{r} \right) + r(y_p - y_r).$$

Obviously, the end points of arc  $K$  satisfy (8); thus

$$(10) \quad (x_p - x_0)^2 + (y_p - y_0)^2 = r^2$$

and

$$(11) \quad (x_r - x_0)^2 + (y_r - y_0)^2 = r^2.$$

Assuming the value of  $T_{yK}$  to be given, we have seven parameters  $x_0, y_0, x_p, y_p, x_r, y_r$  and  $r$  in equations (9)–(11), therefore any four of them may be fixed arbitrarily and then we can calculate the remaining three unknown ones. We may assume, for example, to coincide the end points of both arcs  $K$  and  $\tilde{\Gamma}$ ; then we have to calculate only  $x_0, y_0$  and  $r$  (Fig. 4a). If the arc  $\tilde{\Gamma}$  is symmetrical with respect to the  $x$ -axis, then it consists of some part of  $\Gamma$  and of its reflection in the  $x$ -axis; we have then (Fig. 4b)  $x_p = x_r, y_p = -y_r, y_0 = 0$  and it is sufficient to assume numerical values for the coordinates of one of the end points (note that equations (10) and (11) are identical in this case). In every situation the most convenient way to define the arc  $K$  is to compute  $x_0$  and  $y_0$  from equations (10) and (11), and then to consider (9) as an equation with one unknown  $r$ . In virtue of the transcendental form of (9) its numerical solution is very complicated, so we prefer another procedure: Assuming some value of  $r$ , we calculate from (9) the value of  $T_{yK}$ . If the obtained result does not agree with the assumed one, say  $T_{yK}^0$ , we repeat the calculation, starting from another value of  $r$ , till a reasonable approximation of  $T_{yK}^0$  is obtained.

Unfortunately, the performed numerical calculations have shown that the difference between the values obtained for the static moments  $U$  and  $U_K$  of the domains corresponding to the arcs  $\tilde{\Gamma}$  and  $K$ , respectively, is of the same order as the computation error. Therefore we proceed in a different



way and construct a new line  $\Gamma_p$ , called arch curve, having statical moments whose exactness of evaluation depends only on the approximation of  $\pi$ . The definition of  $\Gamma_p$  and some its properties are given in the next section.

**5. The arch curve corresponding to the anti-ellipse.** Let  $\lambda$  and  $x_k$  be the parameters of our anti-ellipse  $\Gamma$ . By the arch curve  $\Gamma_p$  (Fig. 5) we mean the line consisting of two arcs  $K^{(1)}$  and  $K^{(2)}$  of circles satisfying the following conditions:

(i) the radius  $r_1$  of  $K^{(1)}$  is arbitrarily chosen from the interval  $(x_2 - x_k, y_k)$ ; <sup>(2)</sup>

(ii) the centre of  $K^{(1)}$  is the point  $\vartheta_1 = (x_k, 0)$  and the end points of the arc are  $(x_k, r_1)$  and  $(x_k + r_1, 0)$ ;

(iii)  $K^{(2)}$  is part of a circle with radius  $r_2 = 2\lambda - r_1$  and centre  $\vartheta_2 = (x_k, r_1 - r_2)$ ; the end points of the arc are  $(x_k - r_2, r_1 - r_2)$  and  $(x_k, r_1)$ .

It is easily to be seen that the middle angle, say  $2\alpha_j$ , of each arc equals  $\pi/2$  thus the length of  $\Gamma_p$  is  $\pi\lambda$  and equals to the length of  $\Gamma$ . Note that in the common point  $(x_k, r_1)$  both arcs  $K^{(j)}$  have a common tangent parallel to the  $x$ -axis.

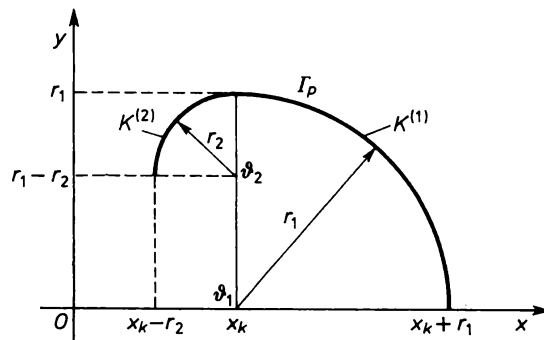


Fig. 5

Let  $S_j = (\xi_j, \eta_j)$  be the centre of gravity of arc  $K^{(j)}$ . According to the well-known formula [5] we have, for  $j = 1, 2$  (Fig. 6),

$$|\vartheta_j S_j| = r_j \frac{\sin \alpha_j}{\alpha_j} = 4r_j \frac{\sin(\pi/4)}{\pi} \quad (3)$$

and therefore

$$\xi_1 = x_k + |\vartheta_1 S_1| \cos(\pi/4) = x_k + 2r_1/\pi,$$

$$\xi_2 = x_k - |\vartheta_2 S_2| \cos(\pi/4) = x_k - 2r_2/\pi.$$

<sup>(2)</sup> According to [7], Figure 7, there is always  $x_2 - x_k < y_k$  except the two extremal cases  $x_k = 0$  and  $x_k \rightarrow \infty$  when the anti-ellipse becomes the arc of a circle.

<sup>(3)</sup> We denote by  $|PQ|$  the length of the segment with end points  $P$  and  $Q$ .

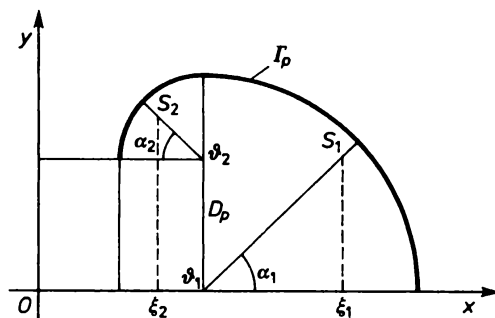


Fig. 6

Denoting by  $l_j$  the length of arc  $K^{(j)}$  we have for the static moment  $T_p$  of the arch line  $\Gamma_p$

$$T_p = l_1 \xi_1 + l_2 \xi_2,$$

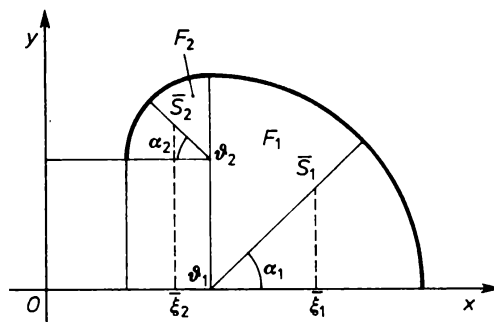


Fig. 7

and this yields after elementary calculation

$$(12) \quad T_p = \frac{1}{2} \pi x_k (r_1 + r_2) + r_1^2 - r_2^2.$$

To compute the static moment  $U_p$  of the domain bounded by  $\Gamma_p$ , by the line  $x = x_k - r_2$  and by the  $x$ -axis (Fig. 7) let us denote by  $\bar{S}_j(\bar{\xi}_j, \bar{\eta}_j)$  the centre of gravity of the domain  $F_j$ ,  $j = 1, 2, 3$ . Then, according to [5], we have

$$|\vartheta_j \bar{S}_j| = \frac{2}{3} |\vartheta_j S_j| \quad \text{for } j = 1, 2.$$

Thus

$$\bar{\xi}_1 = x_k + \frac{4r_1}{3\pi}, \quad \bar{\xi}_2 = x_k - \frac{4r_2}{3\pi}, \quad \bar{\xi}_3 = x_k - \frac{1}{2} r_2.$$

As

$$U_p = \sum_{j=1}^3 \bar{\xi}_j |F_j|, \quad (4)$$

(4) For any plane domain  $D$  we denote its area by  $|D|$ .

similar calculations as above yield

$$(13) \quad U_p = r_1^2 \left( \frac{\pi x_k}{4} + \frac{r_1}{3} \right) + r_2^2 \left( \frac{\pi x_k}{4} - \frac{r_2}{3} \right) + (x_k - \frac{1}{2} r_2)(r_1 - r_2)r_2.$$

Note that the computation error of both statical moments  $T_p$  and  $U_p$  depends only on the error of the assumed approximation of  $\pi$ . The errors corresponding to (12) and (13) are

$$(14) \quad \Delta T_p = \frac{1}{2} x_k (r_1 + r_2) \Delta \pi$$

and

$$(15) \quad \Delta U_p = \frac{1}{4} x_k (r_1^2 + r_2^2) \Delta \pi,$$

respectively.

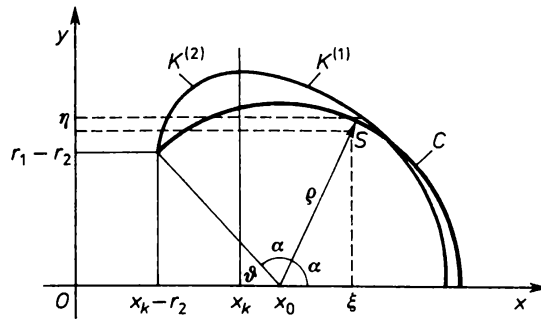


Fig. 8

We introduce now the arc  $C$  of a circle through the following conditions (Fig. 8):

(c<sub>1</sub>) the centre of circle  $\mathcal{G} = (x_0, 0)$  with some  $x_0$ ;

(c<sub>2</sub>) the end point of  $C$  which is closer to the  $y$ -axis is  $(x_k - r_2, r_1 - r_2)$ , the second one lies on the  $x$ -axis; [Note that  $(x_k - r_2, r_1 - r_2)$  is one of the end points of  $\Gamma_p$ .]

(c<sub>3</sub>) the statical moment  $T_C$  of  $C$  equals  $T_p$ .

To define arc  $C$  explicitly we have to calculate its parameters  $x_0$ , the middle angle  $2\alpha$  and the radius  $\rho$ . Denoting by  $S = (\xi, \eta)$  the centre of gravity of  $C$  we have [5]

$$|OS| = \rho \frac{\sin \alpha}{\alpha},$$

thus

$$\xi = x_0 + \frac{r_2}{2\alpha} \sin 2\alpha.$$

The statical moment of  $C$  equals

$$T_C = \xi l_C,$$

where  $l_C$  denotes the length of  $C$ , thus

$$(16) \quad T_C = 2\alpha\varrho x_0 + \varrho^2 \sin 2\alpha.$$

Moreover, we have

$$(17) \quad x_0 = x_k - r_2 + \varrho \cos(\pi - 2\alpha)$$

and

$$(18) \quad [x_0 - (x_k - r_2)]^2 + (r_1 - r_2)^2 = \varrho^2.$$

From equations (16)–(18), where  $T_C$  is given according to (c<sub>3</sub>), we obtain the transcendental equation for

$$(19) \quad \varrho = T_C [r_1 - r_2 + (x_k - r_2 + \zeta)(\pi - \sigma)]^{-1}$$

with

$$\zeta = [\varrho^2 - (r_1 - r_2)^2]^{1/2} \quad \text{and} \quad \sigma = \arcsin \frac{r_1 - r_2}{\varrho}.$$

Equation (19) could be solved approximately using the Taylor expansion of  $\arcsin$ . A more convenient way, applied by the author, is the following one: Let us write (9) in an equivalent form

$$(20) \quad T_C = \varrho [r_1 - r_2 + (x_k - r_2 + \zeta)(\pi - \sigma)].$$

Then, assuming some value of  $\varrho$ , we may calculate  $T_C$  from (20) and compare the obtained result with the given value of  $T_p$ . If the difference between  $T_C$  and  $T_p$  is too great, we may eventually repeat the trial. In this method we treat  $\varrho$ ,  $r_1 - r_2$  and  $x_k - r_2$  as exactly given and calculate the error of  $T_C$ , which equals [9]

$$\Delta T_C = 2\kappa \Delta\pi + \frac{\partial T_C}{\partial \sigma} \Delta\sigma + \frac{\partial T_C}{\partial \zeta} \Delta\zeta$$

with

$$\kappa = \frac{1}{2} \varrho (x_k - r_2 + \zeta),$$

or, after evaluating the derivatives,

$$(21) \quad \Delta T_C = \varrho [(x_k - r_2 + \sigma)(\Delta\pi + \Delta\sigma) + (\pi - \sigma) \Delta\zeta].$$

Moreover

$$\Delta\sigma = \Delta \arcsin \frac{r_1 - r_2}{\varrho} = \Delta \frac{r_1 - r_2}{\varrho} \left[ 1 - \left( \frac{r_1 - r_2}{\varrho} \right)^2 \right]^{-1/2} + \Delta_0,$$

where the first term on the right-hand side is connected with the computation error of the quotient  $(r_1 - r_2)/\varrho$  and the second term follows from the computation error  $\arcsin q$  for a given  $q$ .

The domain corresponding to the arc  $C'$ (Fig. 8) consists of the sector of a circle and of a triangle. Its statical moment is

$$(22) \quad U_C = \frac{1}{3} \varrho^2 (r_1 - r_2) + \frac{1}{2} \varrho^2 (x_k - r_2) (\pi - \sigma) + \frac{1}{2} \varrho^2 \zeta (\pi - \sigma) + \frac{1}{2} (x_k - r_2) (r_1 - r_2) \zeta + \frac{1}{6} (r_1 - r_2) \zeta^2.$$

By similar computations as above we get for the computation error

$$(23) \quad \Delta U_C = \frac{1}{2} \varrho^2 (x_k - r_1 + \zeta) (\Delta \pi + \Delta \sigma) + \left[ \frac{1}{2} \varrho^2 (\pi - \sigma) + \frac{1}{2} (x_k - r_1) (r_1 - r_2) \right] \Delta \zeta.$$

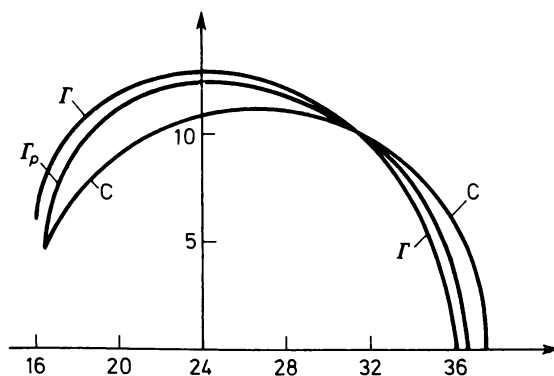


Fig. 9

We illustrate now our investigations by a numerical example. Let us consider the anti-ellipse with extremal abscissas  $x_1 = 16$ ,  $x_2 = 36$  (Fig. 9); then  $\lambda = 10$  and  $x_k = 24$ . The ordinates of the characteristic points are  $y_1 = 6.1582$ ,  $y_k = 13.0844$  and  $y_2 = 0$ . In the arch curve  $\Gamma_p$  we put  $r_1 = 12.5$ ; then  $r_2 = 7.5$ . Assuming  $\pi = 3.14159$  with  $\Delta \pi = 10^{-6}$  we get from (12)

$$T_p = 853.98232,$$

where, according to (14),

$$\Delta T_p = 0.00024,$$

and thus

$$853.98232 - \frac{1}{2} \Delta T_p \leq T_p \leq 853.98232 + \frac{1}{2} \Delta T_p.$$

So we may put

$$(24) \quad T_p = 853.982.$$

Assuming  $\varrho = 11.22$ , we get from (20)

$$T_C = 854.179.$$

For  $\Delta \sigma = 0.0002$  and  $\Delta \zeta = 10^{-4}$  we have from (21)

$$\Delta T_C = 0.004,$$

and so we may put

$$(25) \quad T_C = 854.18.$$

Comparison of (24) and (25) shows that  $T_p = T_C$  with an error less than one. Let us calculate now the statical moments of the corresponding plane domains. From (13) and (15) we get

$$U_p = 5275.3227$$

with an error

$$\Delta U_p = 0.0013.$$

Thus we can put  $U_p = 5275.32$  or, rounding off,

$$(26) \quad U_p = 5275.$$

Using (22) and (23) we obtain

$$U_C = 5175.3$$

with an error

$$\Delta U_C = 0.4,$$

so we may put

$$(27) \quad U_C = 5175.$$

Comparison of (26) and (27) shows that the difference

$$U_p - U_C = 100 > 0$$

is about 2% of the values of both moments  $U_p$  and  $U_C$ , and it exceeds the computation error many times.

It is not hard to see that the arch line  $\Gamma_p$  is closer to the anti-ellipse than the arc  $C$  (Fig. 9). To measure "the error of approximation" we can fix a finite system of abscissas  $x^1, \dots, x^q$  and consider the sums

$$D = \sum_{j=1}^q (y^{(j)} - \eta^{(j)}) \quad \text{and} \quad S = \sum_{j=1}^q (y^{(j)} - \eta^{(j)})^2,$$

where  $y^{(j)}$  and  $\eta^{(j)}$  denote the ordinates of the corresponding points of the anti-ellipse and of the compared line, respectively. Inserting in  $x^{(j)}$  the integers from the interval  $(x, x_2]$  we get in our example for the arch line  $\Gamma_p$

$$D_p = 8.17, \quad S_p = 30.85,$$

and for the arc  $C$

$$D_C = 21.38, \quad S_C = 126.46.$$

**6. Evaluation of the parameters of the anti-ellipse going through a given point.** Suppose we are given an air spring consisting of a flexible nonexpanding shell and fixed on the boundaries of two stiff targets. Assuming rotational symmetry of the air spring, it follows from the author's

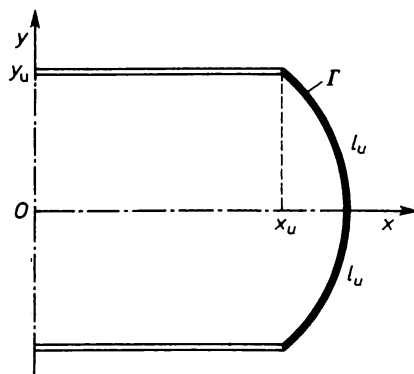


Fig. 10

earlier result [7] that the upper half of the meridian section of the shell lying in the half-plane  $y > 0$  (Fig. 10) is an arc of the anti-ellipse with given length  $l_u$  and going through a given point of fixation  $(x_u, y_u)$ . Now we are led to the following problem: find the parameters  $x_1$  and  $x_2$  of the anti-ellipse using the above mentioned data.

We get from (1) and (5) the system of two equations

$$y_u = \int_{x_2}^{x_u} \frac{x_1 x_2 - x^2}{\sqrt{w(x)}} dx,$$

$$(28) \quad l_u = (x_2 - x_1) \operatorname{arc} \sin \sqrt{\frac{x_2^2 - x_u^2}{x_2^2 - x_1^2}}$$

with two unknowns  $x_1$  and  $x_2$ ; this way of calculating their numerical values is obviously a very inconvenient one. We propose here another method

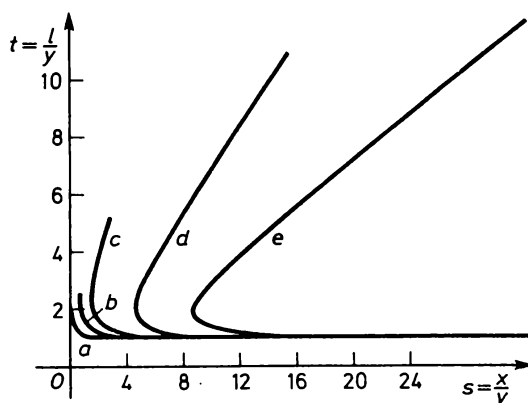


Fig. 11

based on the similarity of the anti-ellipses [7]. Let us put  $s = \frac{x}{y(x)}$ ,  $t = \frac{l(x)}{y(x)}$ , then by equations (1) and (5) every anti-ellipse defines a curve on the  $(s, t)$ -plane (Fig. 11). Note that the curves corresponding to similar anti-ellipses coincide. Each curve starts from the point  $\left(\frac{x_1}{y_1}, \frac{l(x_1)}{y_1}\right)$  and tends to  $(\infty, 1)$  when  $x \rightarrow x_2$ . On Figure 11 we have sketched five curves corresponding to the anti-ellipses with given parameters.

To solve our problem we calculate the values  $s_u = \frac{x_u}{y_u}$ ,  $t_u = \frac{l_u}{y_u}$  and

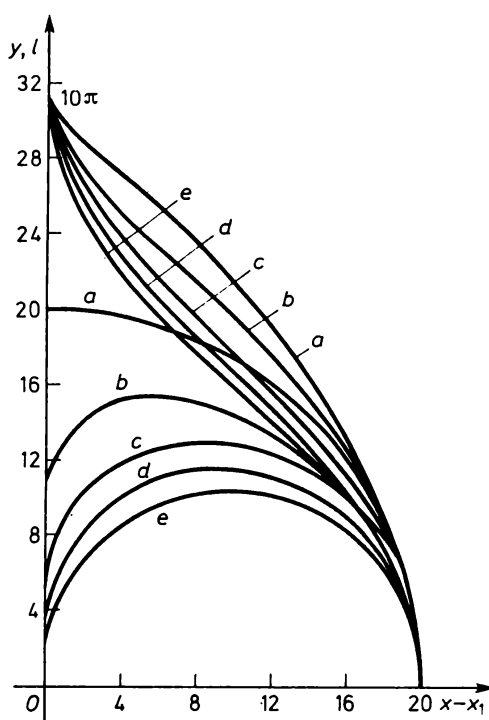


Fig. 12

seek a curve on Figure 11 which goes as near as possible of the point  $(s_u, t_u)$ . We state in this way that the anti-ellipse we are going to find is similar to the one, say  $\hat{l}$ , with given  $\hat{x}_1$  and  $\hat{x}_2$ . It remains only to find the scale constant  $\tau$ . For this purpose we have sketched on Figure 12 the graphs of the functions  $y$  and  $l$ , given by (1) and (5), respectively with identical parameters  $x_1$  and  $x_2$  as used on Figure 11, but expressed in terms of the new independent variable  $\psi = x - x_1$ . To obtain  $\tau$  we choose on Figure 12 the graphs of two functions  $y$  and  $l$  with known parameters  $\hat{x}_1$  and  $\hat{x}_2$ , and seek such a value  $\hat{\psi}_u$  on the  $\psi$ -axis that the identities

$$\frac{\hat{x}_1 + \hat{\psi}_u}{\hat{y}(\hat{\psi}_u)} = s_u, \quad \frac{\hat{l}(\hat{\psi}_u)}{\hat{y}(\hat{\psi}_u)} = t_u$$



hold. Now we have  $\hat{x}_u = \hat{x}_1 + \hat{\psi}_u$ , and

$$(29) \quad \tau = x_u / \hat{x}_u$$

is well defined.

EXAMPLE. Given  $l_u = 27$ ,  $x_u = y_u = 21$ , we have  $s_u = 1$ ,  $t_u = 1.28$  and we can see from Figure 11 that the point  $(s_u, t_u)$  is close to the curve with parameters  $\hat{x}_1 = 5$ ,  $\hat{x}_2 = 25$ . From Figure 12 we find  $\psi_u = 10$ , and  $\tau = 1.4$  according to (29). So the meridian cross-section of the considered air spring is an arc of the anti-ellipse with parameters  $x_1 = 7$ , and  $x_2 = 35$ .

Instead of the above described method we may find approximately the parameters  $x_1$  and  $x_2$  in the following way: Let us suppose that the meridian cross-section of our air spring is the arc of a circle  $K$  (Fig. 13) joining the

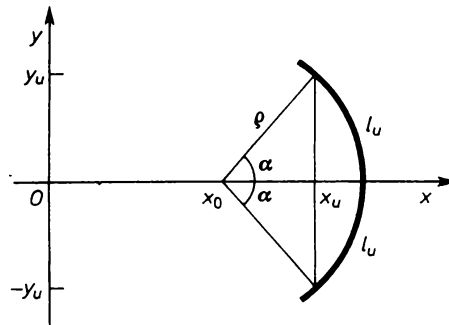


Fig. 13

points  $(x_u, y_u)$  and  $(x_u, -y_u)$ , of length  $2l_u$  and with middle angle  $2\alpha$ . The two unknowns,  $\alpha$  and radius  $\rho$ , of  $K$  may be found from the equations  $y_u = \rho \sin \alpha$  and  $l_u = \rho\alpha$ . Denoting by  $x_0$  the abscissa of the centre of  $K$  (it obviously lies on the  $x$ -axis) we have now  $x_0 = x_u - \rho \cos \alpha$ . Thus  $K$  intersects the  $x$ -axis in  $x_2 = x_0 + \rho$  and the value of the parameter  $x_1$  can be found from (28). The computation error of  $x_1$  and  $x_2$  found in this manner does not exceed 5% if  $x_u > x_k$ ; moreover it does not exceed 1% if  $x_u/\lambda \geq 3.5$ . In the above considered example we obtain  $\rho = 22.7$ ,  $x_0 = 12.38$  and  $x_2 = 35.08$ , instead of  $x_2 = 35$  computed by the first method.

**7. Comparison of the tensions of ring-shaped shells with anti-elliptic or circular sections.** Let us consider a solid consisting of a flexible non-expanding shell, being a ring-shaped fold bounded by two stiff plane targets. Suppose that on this solid acts an external force  $P$  and that there is an overpressure  $p$  inside (Fig. 14). If this solid is an air spring, we have to make the following assumption: The increase of  $p$ , while the force  $P$  remains constant, yields a growth of the height of the air spring. This assumption is correct for all air springs, but not for an arbitrary vessel bounded by a shell. Let us consider for instance a cylinder of height  $l$  having two stiff bottoms with radius  $R$  and suppose its side-shell is made from texture with a non-

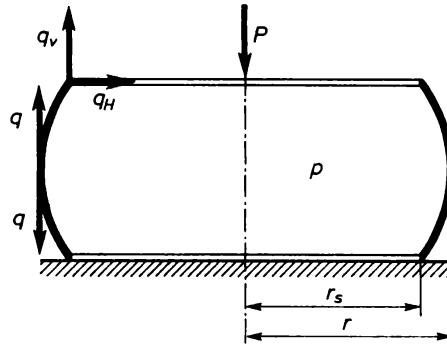


Fig. 14

expanding part parallel to the axis of the cylinder and with an expanding part. Let us suppose also that this shell may bear small loads, conserving its cylindrical shape if there is no overpressure inside. If we let the inside pressure grow, the vessel becomes a barrel and its height  $h$  gets less than  $l$  (Fig. 15). The quotient  $h/l$ , corresponding to the maximal volume, depends on the quotient  $R/l$ .

The air spring connected with an air system is always charged, at least by the empty car body. The overpressure  $p$  in it is balanced by the tension  $q$  of the shell and by the external charge  $P$ ; thus

$$(30) \quad P + 2\pi r q = \pi r^2 p + 2\pi r_s q_v,$$

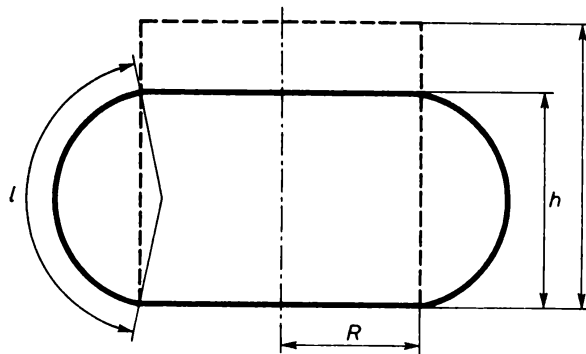


Fig. 15

where  $q_v$  is the vertical component of the tension induced by fixing the shell on the boundary of a stiff target with radius  $r_s$ . For the sake of simplicity let us consider the special case when the meridian of the fold is a half circle  $K$  with radius  $\varrho$  (Fig. 16). Denoting by  $r_0$  the distance of the centre of  $K$  from the axis of rotation we have

$$q_v = 0$$

and

$$(31) \quad r_s = r_0 = r - \varrho.$$

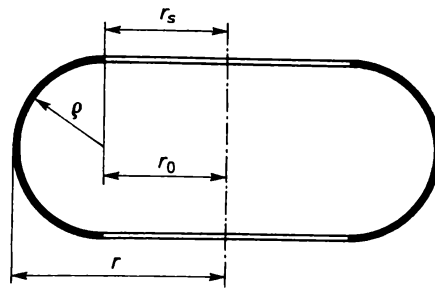


Fig. 16

As the overpressure  $p$  is balanced by the external charge, so

$$(32) \quad P = \pi r_0^2 p.$$

It follows from (30) and (32) that

$$(33) \quad q = \frac{p(r^2 - r_0^2)}{2r}.$$

The obtained result (33) is the same as in the case when the shell is a whole ring surface. Using (31) we may write it in a different form, namely

$$(34) \quad q = p\rho \left(1 - \frac{\rho}{2r}\right).$$

Note that (34) is also true for unbounded shells, if  $r$  and  $\rho$  denote the radius of curvature of the parallel and meridian cross-sections, respectively [10].

Formulas (33) and (34) describe the tension  $q$  rending the shell in its parallel plane. The tension  $q_p$  rending the shell in the meridian plane may be obtained from the known formula

$$\frac{q}{\rho} + \frac{q_p}{r} = p$$

(see [8] and [10]) which yields

$$(35) \quad q_p = p\rho/2.$$

Let us suppose now that the meridian of the considered fold is not an arc of a circle but an arc  $\bar{\Gamma}$  of the anti-ellipse consisting of an arc of  $\Gamma$ , described by (1) with  $x \in (x_k, x_2)$ , and of its reflexion in the  $x$ -axis. In this case we may adapt formulas (34) and (35) with  $\rho$  replaced by  $R_2 = R(x_2)$  (see [7]) and  $r = x_2$ , and we get for the corresponding tensions

$$(36) \quad \bar{q} = pR_2 \left(1 - \frac{R_2}{2x_2}\right)$$

and

$$(37) \quad \bar{q}_p = pR_2/2.$$

After division it follows from (34)–(37) that

$$(38) \quad \frac{\bar{q}}{q} = \frac{rR_2}{x_2 \varrho} \cdot \frac{2x_2 - R_2}{2r - \varrho}$$

and

$$(39) \quad \frac{\bar{q}_p}{q_p} = \frac{R_2}{\varrho}.$$

To compare numerically the tensions in both considered cases let us suppose that the centre of the half-circle  $K$  is  $(x_k, 0)$  and that both arcs  $K$  and  $\bar{I}$  have the same length. Then we have, according to formulas (2) and (5),

$$\frac{\pi}{2} \varrho = (x_2 - x_1) \arcsin \sqrt{\frac{x_2}{x_1 + x_2}},$$

and, as one can see from Figure 16,

$$r = x_k + \varrho.$$

Numerical calculations show that

$$1 \leq \bar{q}/q \leq 1.1 \quad \text{and} \quad 1 \leq \bar{q}_p/q_p \leq 1.15.$$

The values of both considered ratios (38) and (39) depend on the excentricity  $m$  of the anti-ellipse defined as

$$m = \frac{x_1 + x_2}{2} - \sqrt{x_1 x_2}.$$

Its geometrical meaning was described in [7].

In technical realizations the admissible tension of the shell may be always assumed much greater than this one which results from the pressure in the air spring [6]. Therefore it is of no significance if we assume in practical computations the meridian cross-section to be the arc of a circle instead of treating it as a part of the anti-ellipse.

**8. Some additional properties of the anti-ellipse.** The geometrical parameters  $x_1$ ,  $x_2$  and  $x_k$  of the anti-ellipse can be easily expressed in terms of the excentricity  $m$  and of the half-diameter  $\lambda$ . We have

$$x_1 = \frac{(\lambda - m)^2}{2m}, \quad x_2 = \frac{(\lambda + m)^2}{2m}, \quad x_k = \frac{\lambda^2 - m^2}{2m},$$

and

$$x_2 - x_k = \lambda + m, \quad x_k - x_1 = \lambda - m.$$

If the arc of the anti-ellipse corresponding to  $x \in [x_k, x_2]$  is substituted by the

quarter of a circle having the same length  $l_k$ , then the radius  $\varrho$  of this circle equals obviously

$$\varrho = \frac{2}{\pi} l_k$$

with

$$l_k = (x_2 - x_1) \operatorname{arc} \sin \sqrt{\frac{x_2}{x_2 + x_1}}$$

according to (6), and satisfies the inequality

$$x_2 - x_k < \varrho < y_k.$$

As it was shown in [7] in the two extreme cases  $x = 0$  and  $x \rightarrow \infty$  the anti-ellipse<sup>(5)</sup> with given diameter  $2\lambda$  is the half of a circle or a whole circle, respectively. In the remaining situations when  $x \in (0, \infty)$  it may be considered as a deformed circle and,  $\lambda$  being fixed,  $m$  gives the measure of this deformation. The graphs of  $x_2 - x_k$ ,  $y_1$ ,  $y_k$  and  $R_2 = R(x_2)$  considered as functions of  $m$ , with fixed  $\lambda = 10$ , are sketched on Figure 17.

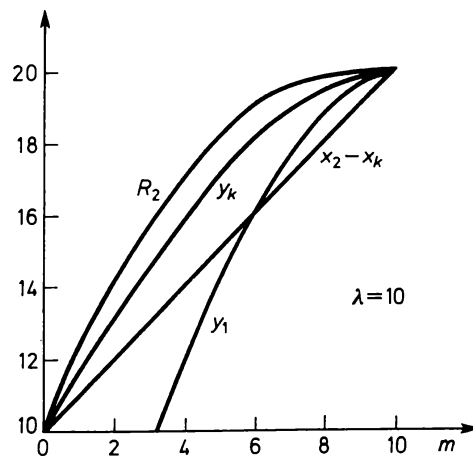


Fig. 17

**9. Final remarks.** It has been shown in this paper that the difference between the anti-ellipse and the circular profile of the deformed fold is insignificant. The substitution of the anti-elliptic profile by a circular one has also no serious influence on the calculated value of the tension of the shell.

Let us note that we have supposed in our considerations the shell to be perfectly flexible, which is not exact and besides the temporary profile of the shell depends on its initial shape ([1] and [11]). The initial profile of the fold is always a circular one.

<sup>(5)</sup> By the *anti-ellipse* we mean now the line consisting of  $\Gamma$  and of its reflexion in the  $x$ -axis.

The anti-elliptic profile may be observed for instance when a child presses on a big soft ball, but this situation is obviously not important in technical applications. Thus in practical investigations one may assume with good accuracy the meridian cross-section of the free part of the shell of an air spring to be the part of a circle.

#### References

- [1] R. A. Akolyan (Р. А. Аколян), *Пневматическое поддрессование автотранспортных средств*, часть 1, Львов 1979.
- [2] L. E. Elsgolc (Л. Э. Эльсгольц), *Вариационное исчисление*, Москва 1958.
- [3] G. M. Fichtenholc (Г. М. Фихтенгольц), *Курс дифференциального и интегрального исчисления*, vol.2, Москва 1948.
- [4] J. Jahnke, F. Emde, and F. Lösch, *Tafeln höherer Funktionen*, Stuttgart 1960.
- [5] J. Leyko, *Mechanika ogólna*, vol. 1, Warszawa 1978.
- [6] J. Marcinkowski, *Elementy usprężynowania I*, Pojazdy Szynowe (1977), no. 1, p. 15-24.
- [7] —, *Geometry of the free part of the shell of an air spring*, Zastos. Mat. 18 (1983), p. 297-309.
- [8] W. Moszyński, *Wykład elementóv maszyn*, Cz. I, Połączenia, Warszawa 1953.
- [9] W. Pogorzelski, *Zarys rachunku prawdopodobieństwa i teorii błędóv*, Warszawa 1952.
- [10] S. Timoshenko and S. Woinowsky-Krieger, *Teoria płyt i powłok*, Warszawa 1962.
- [11] W. Wojno, *Zawieszenia pneumatyczne w pojazdach drogowych*, Warszawa 1962.

INSTITUTE OF MACHINE DESIGN AND OPERATION  
TECHNICAL UNIVERSITY WROCLAW  
50-370 WROCLAW

Received on 8. 7. 1982

---